

The Large Synoptic Survey Telescope: Projected Near-Earth Object Discovery Performance

Steven R. Chesley
Jet Propulsion Laboratory
California Institute of Technology
Pasadena, CA 91109
steve.chesley@jpl.nasa.gov

Peter Veres
Jet Propulsion Laboratory
California Institute of Technology
Pasadena, CA 91109
peter.veres@jpl.nasa.gov

Abstract—The Large Synoptic Survey Telescope (LSST) is a large-aperture, wide-field survey that has the potential to detect millions of asteroids. LSST is under construction with survey operations slated to begin in 2022. We describe an independent study to assess the performance of LSST for detecting and cataloging near-Earth objects (NEOs). A significant component of the study will be to assess the survey’s ability to link observations of a single object from among the large numbers of false detections and detections of other objects. We also will explore the survey’s basic performance in terms of fraction of NEOs discovered and cataloged, both for the planned baseline survey, but also for enhanced surveys that are more carefully tuned for NEO search, generally at the expense of other science drivers. Preliminary results indicate that with successful linkage under the current baseline survey LSST would discover $\sim 65\%$ of NEOs with absolute magnitude $H < 22$, which corresponds approximately to 140 m diameter.

TABLE OF CONTENTS

| | | |
|---|----------------------------|---|
| 1 | INTRODUCTION | 1 |
| 2 | KEY STUDY ELEMENTS | 2 |
| 3 | BASELINE PERFORMANCE | 6 |
| 4 | MOPS TESTING | 7 |
| 5 | SUMMARY | 8 |
| | ACKNOWLEDGMENTS | 8 |
| | REFERENCES | 8 |
| | BIOGRAPHY | 8 |

1. INTRODUCTION

The Large Synoptic Survey Telescope (LSST) is an ambitious project that has the potential to make significant contributions to Near-Earth Object (NEO) search efforts. LSST is jointly funded by the National Science Foundation and the Department of Energy, with significant enabling contributions from private donors. Construction is already underway and major optical elements are complete. Figure 1 depicts the telescope and dome design in cutaway. LSST first light is set for 2020, followed by two years of commissioning. Once regular survey operations begin in 2022, LSST will systematically survey the observable sky over a ten-year period from its site on Cerro Pachon, Chile.

With an 8.4 m aperture (6.7 m effective), 9.6 square degree field of view, and a 3.2-Gigapixel camera, LSST has the potential to become the world’s most capable asteroid survey instrument. LSST will be able to cover over 6000 square degrees of sky per clear night with single visit exposures of 30 s, reaching a faint limit of 24.5 mag in the r band [1]. The survey’s search cadence, however, is a critical factor for NEO

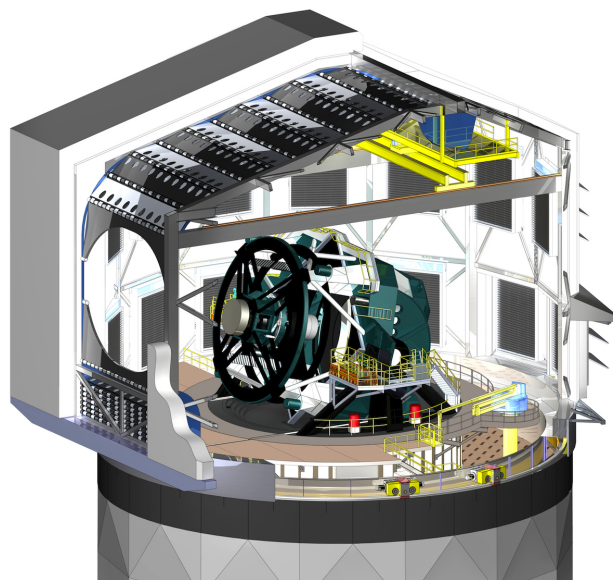


Figure 1. A computer rendering of the baseline design of the LSST dome with a cutaway to show the telescope within. Image Credit: LSST.

discovery performance, and there are multiple science drivers whose different cadence needs are being discussed and will eventually be balanced to shape the final survey strategy.

We are conducting a study to examine the NEO search performance of various LSST search strategies, paying particular attention to the challenges of linking large numbers of asteroid detections in the presence of false detections. Our approach is to derive lists of synthetic detections for a given instantiation of the LSST survey, based on an assumed model for the populations of solar system objects from the main asteroid belt inwards to the near-Earth population. These detection lists are combined with false detection lists that model both random noise and non-random artifacts resulting from image differencing algorithms. These voluminous detection lists are fed to the Moving Object Processing System (MOPS) [2], which attempts to link the synthetic detections correctly without becoming confused or overwhelmed by the false detections.

The LSST baseline survey cadence relies primarily on single night pairs of detections, with roughly 30 minutes between the elements of a detection pair. These pairs form what are known in MOPS parlance as *tracklets*, and sets of tracklets are linked across multiple nights to form *tracks*, which can then be sent to the final step, which is orbit determination. The strategy of using pairs is an aggressive and potentially fragile

approach, but theoretically represents the most productive NEO search with the minimum impact on other LSST science drivers. An alternative to visit each field three times per night to form tracklets from triplets of detections may prove more robust, but likely with a penalty of reduced performance. One of our study objectives is to understand the tradeoffs between these two approaches.

While we strive for an independent study, we do intend to collaborate with LSST and other organizations, e.g., IPAC (Caltech’s Infrared Processing and Analysis Center), to the extent that cooperation will improve the study results and ensure their broad acceptance by stakeholders and the community at large. In particular, we intend to rely on LSST for certain key inputs that would be inappropriate or impractical to derive independently. Similarly, we must ensure that our study uses assumptions and inputs that are in accord with those used by the LSST project. Moreover, as LSST progresses with their own validation efforts, we plan to ensure that our respective results are directly comparable, e.g., by using the same input data streams. This “semi-collaborative” footing will allow the JPL-led study to progress more quickly and afford independent validation of key results. Additionally, any identified discrepancies can be cleared more readily through open communication and sharing of inputs.

2. KEY STUDY ELEMENTS

The two major questions to be addressed by our study can be informally stated as “Will MOPS work?” and “If MOPS works what fraction of NEOs will LSST discover?” The first question revolves on the linkage problem and the risk of confusion and an ensuing combinatoric crisis in computation. Indeed, the central challenge for the LSST NEO survey is the linking problem, where putative detections of individual moving objects are combined, first within each night, and then across multiple nights, thereby confirming with high confidence that a moving object has been detected and allowing the associated orbit to be computed and cataloged.

The second question is addressed by quantifying the completeness of the NEO catalog produced by LSST, i.e., the fraction of solar system objects in a given population and size range that LSST would find. Completeness comes in two types, differential completeness, which refers to a given (presumably narrow) size bin, and integral completeness, referring to all objects larger than some given size. Our primary metric for LSST NEO performance is the integral NEO discovery completeness for absolute magnitude $H < 22$, though there are a number of other metrics related to, for example, the quality of the orbits of the discovered objects.

Both questions require a high-fidelity asteroid detection model to reach an answer, but the actual approach is markedly different between the two. For the linkage problem we must test MOPS in the presence of confusion due to NEOs, Main-Belt Asteroids (MBAs) and false detections. Thus we must generate full-density detection lists and then feed these lists to the linking engine. The number of detections entering the pipeline must match the expected data load of the real LSST, and subtle details in the detection model are less important than assuring the anticipated volume of detections. Thus MOPS testing entails the most computational stressing part of the study, but fortunately the full-density simulations need only take place over ~ 3 observing cycles (also called lunations or dark runs) to understand the MOPS performance. This means that only a tiny fraction of the 10-year survey

need be simulated to understand whether MOPS will perform successfully.

In contrast, to obtain the end-of-survey NEO completeness we must run the entire 10-year survey. However, we can assume that MOPS will be tested elsewhere, and so we do not need a full-density detection list, nor do we even need to run MOPS. In fact, only the NEO population need be included in the simulation; noise and MBAs can be neglected. Moreover, a sampling of only a few thousand NEOs is adequate to answer the question. But while the computational load for completeness testing is quite manageable, the fidelity of the detection model becomes crucial.

With this background in mind, we now turn to a discussion of the key simulation elements that form the framework of the study.

Operational Simulator

LSST’s Operational Simulator (OpSim) tool [3] uses project scheduling tools to compute all of the field pointings and ancillary information for a full-length, high-fidelity survey, comprising ~ 2.5 million individual field visits over ten years. OpSim models include realistic weather, seeing, sky background noise, etc. For our purposes, the essential OpSim output is a field-by-field listing of the pointings, camera rotation angles, filter selections and the SNR=5 limiting magnitudes M_5 .

We will use the outputs of OpSim runs as inputs to our study, and we do not envision generating our own OpSim runs. Our initial focus is the current LSST baseline OpSim run, designated “enigma_1189”, although we expect that the project will continue to revise its baseline during the course of the study. We anticipate that special purpose (e.g., NEO-optimized) OpSim runs will be run by LSST for its own needs, and indeed some of these have already been completed. We also anticipate that the LSST project will produce any additional OpSim runs that are judged critical for our study, though the details of any such runs will need to be negotiated once their purpose and parameters are understood.

Solar System Model

For NEOs we are using the Bottke population model [4], as published by Grav et al. [5]. The model includes a full population of 270,000 NEOs down to $H = 25$ (~ 35 m diameter for a 14% albedo sphere). Note that objects fainter than $H = 25$ will be detected by LSST, but the sky-plane rates of motion will often be too high and the areal density of such objects is expected to be low. We will revisit the question of the appropriate lower size bound on the NEO model as our study progresses, although the primary reason for doing so would be to understand completeness at very small sizes (< 50 m), which we do not consider as a crucial performance metric. We intend to test NEO completeness with the NEO model developed by Granvik et al. [6] after it becomes publicly available.

For the main-belt asteroids (MBAs) we use the model published by Grav et al. [5], which includes 14 million MBAs with apparent magnitude $V < 24.5$ when at both perihelion and opposition. We recognize that LSST should be able to detect some MBAs somewhat fainter than this, and we will evaluate the impact of this gap as our study progresses. The primary reason for including the MBAs is to properly model the confusion problem, and if we find that it is necessary from this perspective to extend the Grav MBA model to fainter

limits then we will do so.

For completeness estimates, we need only run ~ 2000 model NEOs, all with a single absolute magnitude value, through the simulated survey. Post-processing will allow us to accurately derive key metrics, such as completeness and the distribution of arc length, at a range of sizes and from there obtain, e.g., integral completeness for $H < 22$.

Focal Plane Model

An accurate model of the LSST focal plane is required as a first step in developing high-fidelity detection lists. Figure 2 is a schematic diagram of the LSST focal plane, which consists of 21 CCD rafts with each raft comprising a 3×3 array of $4k \times 4k$ CCDs. Thus there are a total of $21 \times 9 = 189$ CCDs. There are also guide and wavefront sensor CCDs in the corners of the focal plane, but we assume they are not useable for NEO detections. Our modeling approach for the focal plane leverages existing the MOPS formulation, which allows either a square or circular field and allows masking of square sub-regions within the field. We model LSST as a square focal plane with a 5×5 array of rafts and mask the four corner rafts. The LSST focal plane will take different orientations and so we rotate this partially masked focal plane as shown in Fig. 3.

We also need to account for the raft gaps and the smaller chip gaps within each raft. While the exact dimensional specifications for LSST focal plane are not yet finalized, our approach assumes each raft occupies a focal plane area of $(2500 \text{ arcsec})^2$ and within each raft area the CCD area is $(2400 \text{ arcsec})^2$, which is in accordance with the current baseline focal plane design. With these assumptions we find a focal plane fill factor of $F_{\text{fill}} = 92\%$, which is the fraction of focal plane area that is covered with active CCD pixels. Our current study approach is to statistically under-sample detections, both synthetic and false, according to the fill factor.

Figure 4 depicts a full LSST field with a full-density NEO and MBA model plus random noise. This field is near the ecliptic plane and near opposition in good conditions and so it represents the highest density of real objects likely to be seen by LSST. For this reason the figure shows an unusually low fraction of false detections: 14% of the 4800 total detections in this field are random noise and the rest are from synthetic detections. Fields far from the ecliptic will be dominated by noise because of the low density of detections. However, as discussed in Sec. 4, in the mean across the full range of observing circumstances the number of false detections from random noise should be roughly similar to the number of detections from solar system objects.

Synthetic Detections

We simulate detections of moving objects by joining a given OpSim run, which is a detailed image-by-image instantiation of a ten-year LSST survey, with a synthetic Solar System Model (SSM) of NEOs and MBAs. Given the observing circumstances of each field visit, we ascertain which SSM objects in the field are bright enough to be detected. This allows us to assemble a list of synthetic detections of moving objects over the duration of the survey. The following modeling details are relevant for generating the detection lists.

a) Trailing losses. Moving objects trail across multiple pixels, which makes them harder to detect than stationary objects. In the best case one can implement a trail or streak detection

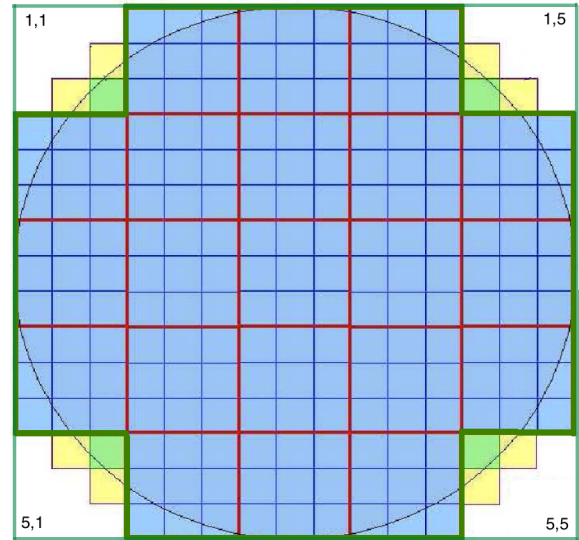


Figure 2. Schematic of the LSST focal plane. The heavy green lines indicate the boundaries of the detection area. The red squares represent the CCD rafts and the small blue squares represent individual CCDs

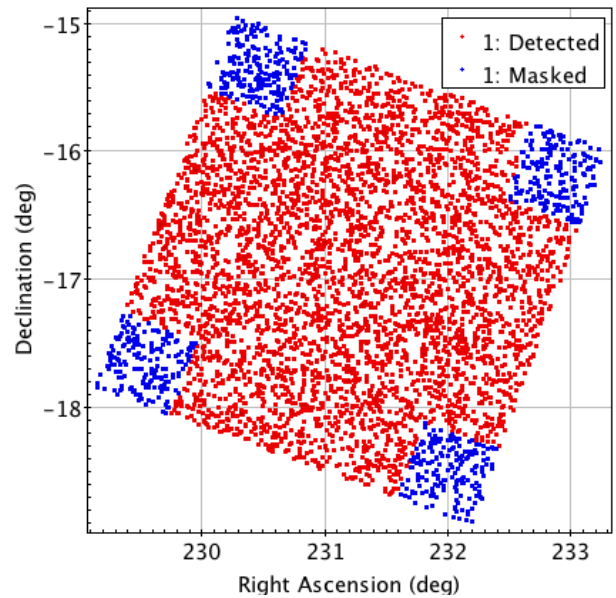


Figure 3. Depiction of detections and masking for a rotated field. Position Angle (PA) in this example is 20° (angle of rotation from North towards East).

algorithm that sums the signal along the whole streak to compute the SNR and decide if the detection is significant. LSST does not plan to identify sources through trail detection, but rather will use a circular PSF detection kernel, which will only capture the signal within the seeing disk. Thus long trails will only be detected when they have a high enough signal in a seeing disk, which may cover only a short subsegment of the trail. Figure 5 depicts the rate of motion of NEOs seen in the baseline LSST survey. For a $2^\circ/\text{day}$ rate of motion, a moving object will move 2.5 arcsec in a single 30 s visit, which is ~ 3 seeing disks under typical conditions.

Streak detection entails an SNR loss due to the fact that the asteroid signal is spread across more pixels, thus picking up

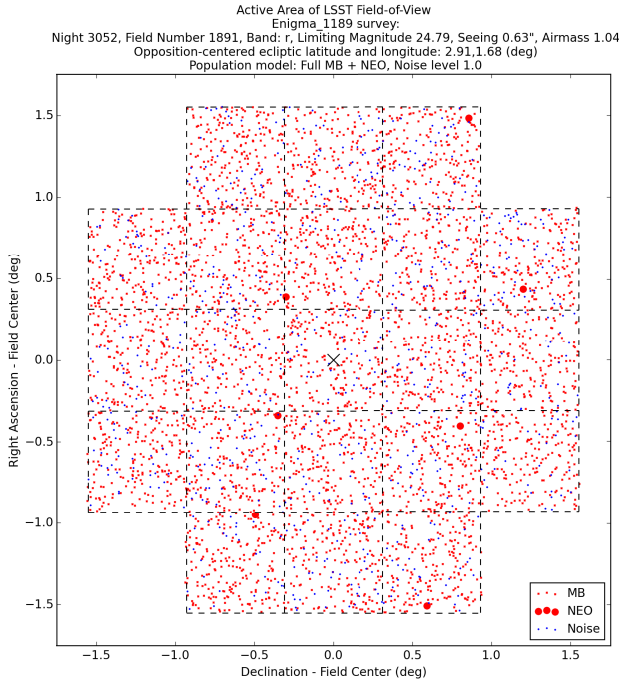


Figure 4. Detections from a single LSST field, including NEOS, a full-density main asteroid belt and random noise. There are 762 false detections and 4038 asteroids, including 7 NEOs. Field rotation angle is set to zero for this example.

more background noise with the same signal. The limiting magnitude loss for such cases is given by the lower curve in Fig. 6, while the more severe LSST detection losses ΔM_5 are given by the upper curve, according to

$$\Delta M_5 = 1.25 \log \left(1 + a \left(\frac{vt}{s} \right)^2 \right),$$

where $a = 0.42$ is an empirical constant, v is the rate of motion of the asteroid, t the exposure time and s the seeing (L. Jones, private communication). We note that if LSST does make a detection through the point source detection algorithm then the return will be convolved with a trail-fitting algorithm to extract the rate and direction of motion, which is vital information for linking fast-moving objects.

b) Detection fading. Rather than assuming a step function cutoff at the M_5 faint limit, we assume a more realistic gradual fading, where the probability of making a detection falls smoothly from $\sim 100\%$ to zero in an interval (~ 1 mag wide) surrounding M_5 . More specifically, fill factor and fading are applied simultaneously in a single test where each synthetic detection is accepted if

$$R < \frac{F_{\text{fill}}}{1 + \exp\left(\frac{m - M_5}{w}\right)}, \quad (1)$$

where $0 \leq R < 1$ is a random number drawn from a uniform distribution, m is the apparent magnitude of the asteroid, M_5 is the limiting magnitude of the observed fields and $w = 0.1$ is a fixed fading factor. This fading model is depicted in Fig. 7 where we demonstrate that the computed fading and fill factor losses match the desired model. We note that, because there are more detections as the apparent magnitude grows fainter

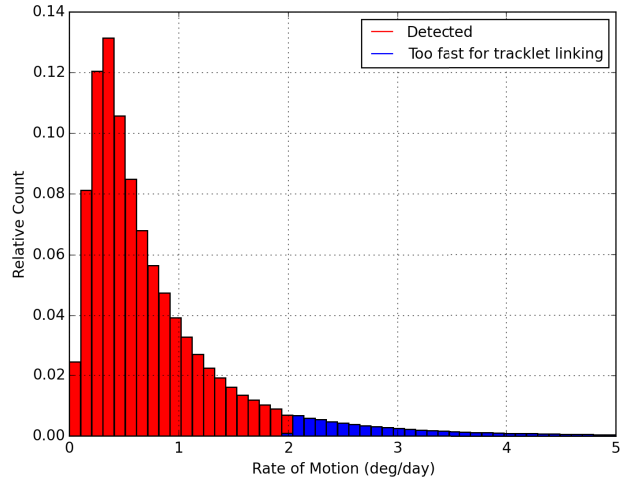


Figure 5. Histogram of plane-of-sky rates for NEOs detected by LSST in one year. Our default rate cutoff of $2^\circ/\text{day}$ leads to a loss of 7.1% of potential detections.

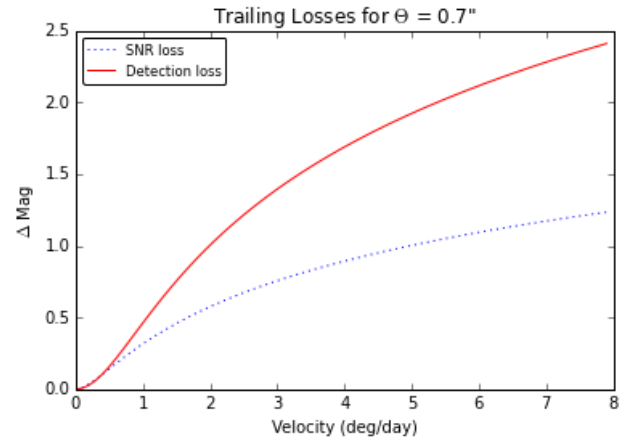


Figure 6. Tailing losses in magnitudes for 0.7 arcsec seeing. LSST will experience losses given by the “Detection loss” curve, while implementation of a streak detection algorithm could reduce the losses to that of the “SNR loss” curve. Image Credit: L. Jones, (LSST/Univ. Wash.)

(Fig. 8), implementation of a fading model actually increases survey performance slightly, with a gained-to-lost ratio of 1.2.

c) Asteroid colors. Asteroids have a varied taxonomy, with each taxon having its own set of color indices that affect the apparent brightness in the different LSST filters. This means that the detectability of a given real-world asteroid will depend upon its color index. We intend to implement a number of asteroid taxa and associated color indices as an added level of fidelity, although this has not yet been done.

d) Light curves. Asteroids are not uniform, spherical bodies, and so as they rotate their apparent brightness varies, primarily due to their irregular shapes. This “light curve” variation can often be a few tenths of a magnitude and occasionally even more than 1 mag. The obvious implication is that some asteroids may rise above and fall below the detection threshold during a sequence of observations, and so some detections might be lost and others gained as compared to the assumption of constant absolute magnitude. The effect this

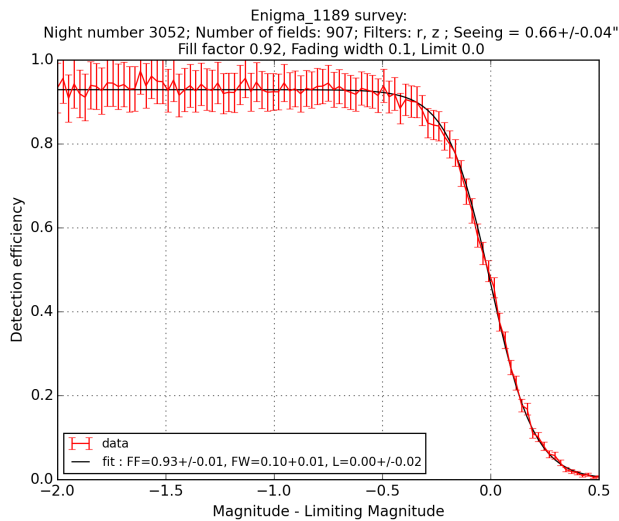


Figure 7. Validation of focal plane loss model for 907 fields in a single night. The detection model calls for a smooth fading across the SNR=5 limiting magnitude, where we have 50% probability of detection, convolved with a 92% fill factor.

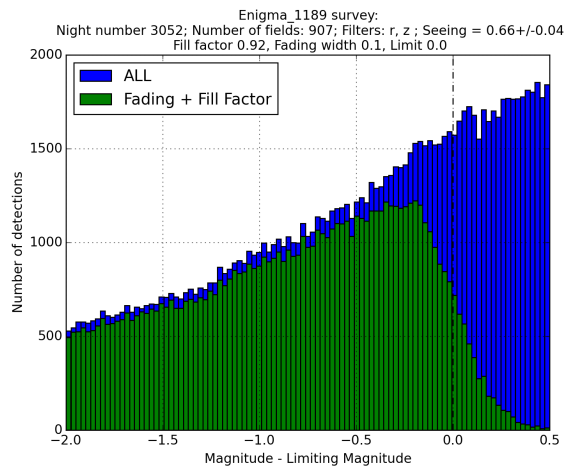


Figure 8. Depiction of our detection model. Initially all detections up to 0.5 mag fainter than the SNR=5 limiting magnitude are retained. Then fading and fill factor losses are removed (blue), leaving the simulated detections (green).

has upon the survey performance is presumed small, but has yet to be determined. We expect to include this refinement to our detection model in the course of the study.

Among the foregoing detection modeling aspects, trailing losses clearly have a significant effect on the detectability of moving objects, NEOs in particular, and this is a vital element for both completeness estimates and for MOPS testing. Preliminary tests indicate that fading has only a minor effect on completeness and is irrelevant for MOPS testing. We anticipate that light curves and color corrections will also have a minor effect on completeness estimates, and are likely to be irrelevant for MOPS testing.

False Detections

Spurious detections are an unavoidable element of any asteroid search program. For LSST there will be two distinct

sources of false detections, namely random noise and image differencing artifacts. The easiest to model are those arising from random noise in the detectors, which are randomly distributed with an areal density depending on the Signal-to-Noise Ratio (SNR) of the detection threshold.

The other type of false detection arises from artifacts in the *image differencing* technique that LSST will use to detect moving objects. LSST will build up a deep-stack, fiducial image of the sky, known as a “template sky,” by combining numerous images of the same field. Individual images are then compared to the template sky and sources that are present only in the single visit are considered potential moving objects. This process readily reveals variable but stationary objects (e.g., variable stars) and these will be effectively removed from the detection stream. The process also generates “Difference Image Artifacts” (DIAs) that arise from any number of quirks in the differencing process, e.g., diffraction spikes and imperfect image alignment, to name but two. These can be screened to some extent by machine-learning algorithms, but their areal density in the LSST data stream has not yet been fully characterized. It is important to note that DIAs can be correlated, both within individual images and between pairs of images, and thus their positions can shift between images in a way that can mimic the motion of real solar system objects.

For false detections stemming from random noise we will generate our own lists with an agreed model [7] and collaborators may share or exchange lists to facilitate comparison. For DIAs, we will initially generate lists assuming a random distribution with a range of areal densities to understand the noise loading that causes the linkage engine to falter. The LSST Project is currently using real data, e.g., Dark Energy Camera images, to refine estimates of the rate of DIA creation and understand the effectiveness of DIA rejection techniques. We expect that this effort will provide a more refined model for injecting DIAs, including correlation rules. As our study progresses, we expect that LSST will provide DIA lists for a given OpSim run, which could be directly merged with synthetic and random false detection lists and fed to the linking engine.

We will introduce false detections at a variable rate. Initially we will use only the expected rate of Gaussian noise, but then we will increase this to 2 \times , 5 \times , and perhaps even 10 \times the Gaussian noise rate. The point of increasing the random noise level beyond what is expected is to crudely model the presence of DIAs and to understand where noise starts to compromise MOPS performance.

Linkage

Linking the stream of potential moving object detections generated by LSST is one of the more computationally stressing elements, both for the LSST project and for the current study. The image-by-image, night-by-night data stream of synthetic and false detections is fed to the linking engine, known as the Moving Object Processing System (MOPS), which was jointly developed by Pan-STARRS and LSST, with significant NASA support [2]. MOPS development forked a number of years ago and now there are at least three incarnations that are relevant to our study, namely those in use by Pan-STARRS, LSST and NEO-WISE. For the study we describe here, these are the MOPS versions to be run at JPL, Univ. Washington and IPAC, respectively.

NEO surveys have historically been conducted by searching through nightly sets of 3-5 images, with each image

separated by 30-60 minutes, and looking for objects that show consistent rates of motion in all (or all but one) of the images. Ensuring at least three mutually compatible detections allows a high confidence that the detections are associated with moving objects and are not spurious. In some cases a preliminary orbit estimate can be derived from such a single-night string of detections.

In a marked departure from this traditional approach, LSST plans to capture moving objects from pairs of images taken in a single night (both differenced from a long-duration template sky). They intend to link potential detection pairs (the majority of which may be spurious due to confusion and false detections) over a series of three or more nights to identify real objects and eliminate false detections. This strategy has been shown to work in simulations [2], but has never been operationally demonstrated, increasing the importance of high-fidelity tests and simulations that demonstrate that the approach will indeed perform as intended.

Our approach to the linkage problem will be to use the Pan-STARRS version of MOPS, which is presently the only version with a validated orbit determination process, where the final screening step takes place for computing and cataloging moving objects. This MOPS version uses the JPL orbit determination software package, with which we are well acquainted. Where appropriate, we intend to collaborate closely with both LSST and IPAC to unify MOPS settings and inputs and to compare outputs.

3. BASELINE PERFORMANCE

The *enigma_1189* survey, which is currently designated as the baseline survey, is a strawman survey intended for detailed understanding of the resulting science performance for LSST’s numerous science drivers. Here we first describe the key characteristics of the survey and then we present a preliminary analysis of the NEO survey performance.

Survey description

For *enigma_1189* the available sky is divided into 3339 unique field pointings, or footprints. The baseline survey covers a time span of 10 years, although some nights are removed due to simulated weather patterns. There are 2 469 307 individual field visits from 3062 nights with data. Mean seeing in the survey is 0.80 ± 0.20 arcsec and median seeing is 0.76 arcsec. Mean limiting magnitude per filter is tabulated in Table 1. The total time spent on a visit, including exposure time, CCD read time and slewing, is typically 39–44 seconds. The survey returns to the same part of the sky roughly every 3 or 4 nights.

Table 1. Mean (with standard deviation) and maximum limiting magnitude M_5 of the *enigma_1189* survey in the various LSST filters.

| Filter | Mean M_5 | Max. M_5 | Time spent (%) |
|--------|------------------|------------|----------------|
| u | 23.75 ± 0.37 | 23.75 | 8 |
| g | 24.67 ± 0.37 | 25.53 | 10 |
| r | 24.38 ± 0.36 | 25.21 | 22 |
| i | 23.66 ± 0.38 | 24.57 | 22 |
| z | 22.44 ± 0.42 | 23.89 | 20 |
| y | 21.49 ± 0.25 | 22.11 | 18 |

The *enigma_1189* survey contains 5 distinct “proposals,” i.e., individual surveys with different objectives and cadences

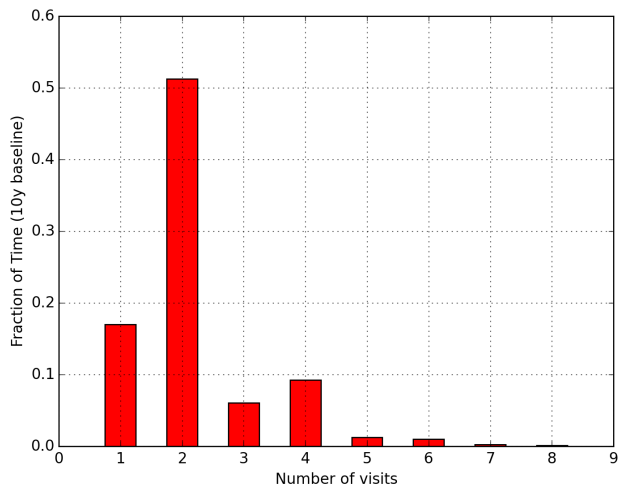


Figure 9. The fraction of LSST survey time in the baseline (*enigma_1189*), according to the number of visits per night (within 2 hours).

that guide the overall survey schedule and design. These proposals receive different fractions of the total survey time as indicated in Table 2. Over 90% of the survey is dedicated to the most productive NEO proposals, namely Universal Survey and Northern Ecliptic Spur.

Figure 9 depicts the fraction of *enigma_1189* time (and fraction of fields) that form a nightly n -tuple for $1 \leq n \leq 8$. More than half of survey time is spent on single-night pairs. The mean time span between first and last visit of an n -tuple is 42 minutes, but $\sim 7\%$ of tuples are longer than 2 hours. Approximately 17% of time is spent on single visit fields that are of no value for NEO discovery. Among these, 64% are in the u and y filters, which have poor performance for detecting NEOs and thus are not scheduled to be executed in nightly pairs. And so only 6% of fields are singletons shot in a filter suitable for NEO discovery. About 4% of the time is spent on Deep Drilling, which is also not suitable for NEO search because it continuously visits one individual field for an extended period (n -tuples with very large n), often for cosmological studies with a purpose of deep stacking.

Table 2. Time spent on various observing “Proposals” for the LSST *enigma_1189* survey.

| Proposal | Time spent (%) |
|----------------------|----------------|
| Universal Survey | 86 |
| North Ecliptic Spur | 6 |
| Deep Drilling | 4 |
| Galactic Plane | 2 |
| South Celestial Pole | 2 |

NEO performance

Figures 10 and 11 provide a preliminary assessment of the NEO search performance with *enigma_1189*. Figure 10 depicts completeness as a function of absolute magnitude for the complete ten-year survey, while Fig. 11 depicts completeness as a function of time for NEOs brighter than $H = 22$. Both plots have five curves representing different completeness metric. These are the fraction of objects with

- at least one detection

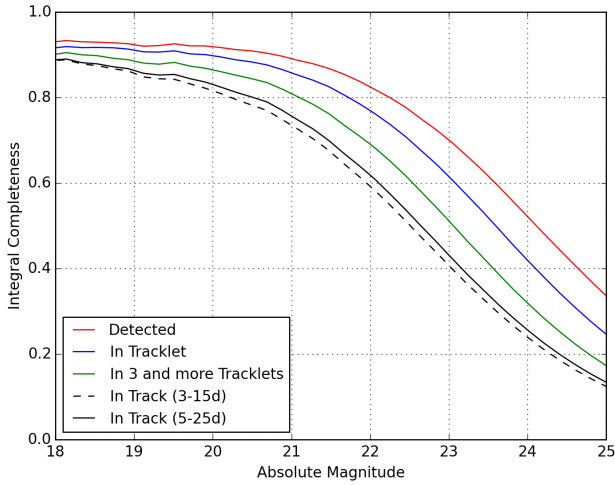


Figure 10. Preliminary results for NEO integral completeness for `enigma_1189` as a function of absolute magnitude H .

- at least one tracklet (two or more detections in a single night with maximum separation two hours)
- at least three tracklets (with no time constraints)
- at least one “3-15” track (three tracklets where a pair of tracklets are separated by ≤ 3 days and a third tracklet is ≤ 15 days from the pair)
- at least one 5-25 track (a pair of tracklets separated by ≤ 5 days with a third tracklet within 25 days of the pair).

The completeness curves reveal the progressive losses as we step from detections to tracklets to tracks, and finally to constrained tracks that we expect MOPS will be able to link and catalog as objects with orbits. We note that the strict 3-15 track requirement leads to only a small degradation in performance relative to the more relaxed (i.e., more challenging for MOPS) 5-25 track requirement. Completeness for $H < 22$ is 59% and 62% for 3-15 and 5-25, respectively. For $H < 25$, about a third of the population is detected, although about half of these are detected only once.

We emphasize that the foregoing discussion and related figures are preliminary and are presented as examples of the kind of results anticipated for the study. We continue to vet and refine the model assumptions and fidelity and as a result the final performance assessment may be different.

4. MOPS TESTING

We intend to move gradually to full-scale MOPS runs. All MOPS tests will use a full NEO population with a rate of motion cutoff at $2.0^\circ/\text{day}$ as a baseline and add additional detections by including MBAs, noise and faster objects. Table 3 provides a notional list of parameter values to be tested:

Table 3. Range of parameters panned for MOPS testing.

| Parameter | Values to be tested |
|-------------------------------------|---|
| MBA model | 0%, 10%, 30%, 100% |
| Gaussian Noise | 0 \times , 1 \times , 2 \times , 5 \times |
| Rate limits ($^\circ/\text{day}$) | 0.5, 1, 2, 5, 10 |

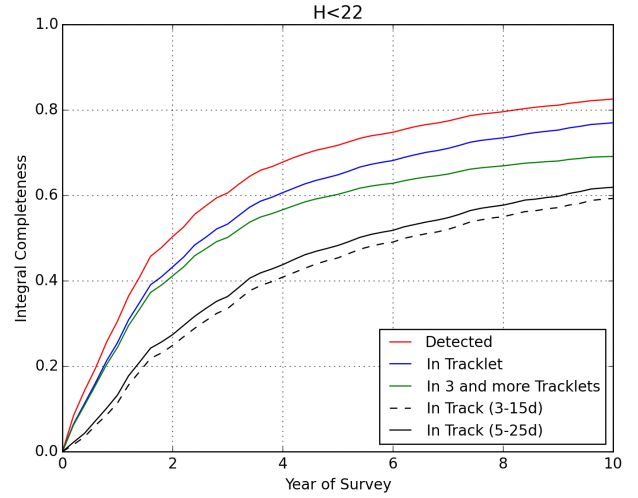


Figure 11. Preliminary results for NEO integral completeness for $H < 22$ for `enigma_1189` as a function of survey duration.

Initially we will focus on run times for single-night tracklet generation, which will guide us in selecting several cases to be run for a whole lunation. The full detection lists for these single lunation runs will be a common input for MOPS runs across the study.

The MOPS runs have three key steps to build a catalog of orbits:

Tracklets: The single lunation detection lists will first be run through the tracklet generation stage to verify scaling of run times as a function of the varied inputs and MOPS tuning parameters. The accuracy and efficiency of tracklet generation will be computed and verified. MOPS tuning parameters are a key element of this comparison.

Tracks: We will next start exploring track generation. Tracks are three tracklets in distinct nights within 15 nights that comply with simple curve fitting requirements. This stage is the most computationally intensive and is highly sensitive to numerous MOPS tuning parameters. This is where the runs must be designed with care. An understanding of the run time scaling is key for selecting the sequence of track generation tests to be run. The first runs will be with only NEOs to ensure that tuning parameters are set correctly to avoid losing NEOs in the simplest case. This will provide a good starting point for optimizing MOPS parameters. Track generation performance and lists will be compared with external study participants.

Orbit Determination: The final step in cataloging an object’s orbit is orbit determination (OD). Here orbits are fit to all candidate tracks and the χ^2 of observation residuals is used as a quality metric to screen false tracks. After this final stage we derive the cataloging accuracy and efficiency metrics. The key performance statistic at this stage is the accuracy (fraction of false orbits) and efficiency (fraction of potential orbits that were cataloged).

As of this writing we have some progress along the path outlined here. In particular, we have completed a full observing cycle (i.e., lunation) with NEOs + 100% MBAs with different levels of random noise. Table 4 lists the statistics for detections and tracklets in this preliminary simulation, which will be refined as our models continue to improve

over the course of the study. This simulation produced ~ 14 million detections and a similar number of false detections with $1\times$ noise, with the real-to-false detection ratio following naturally according to the multiplier applied for the random noise. Tracklet counts, however show a surprising pattern in that for all three noise levels there are approximately 0.3 tracklets per detection. The implication is that the addition of random noise beyond a certain level only leads to a linear increase in the number of tracklets, despite the combinatorial potential for the number of tracklets to grow much faster than linear. This limit in the rate of growth of the number of tracklets is presumably related to the $2^\circ/\text{day}$ rate of motion limit applied in the tracklet formation.

While the number of real tracklets present in the simulation is obviously constant, the total number of tracklets formed grows with the noise level, and so the real-to-false tracklet ratio falls, but for the cases in Table 4 the ratio falls more slowly than linear in the inverse of the noise level, suggesting that high levels of noise do not pose a problem for tracklet generation. The CPU times for tracklet generation were quite manageable in these tests, as shown by the table. Our next major step in the study is to turn to track generation, which is the most computationally expensive.

Table 4. Detections and tracklet statistics for one observing cycle (lunation) of *enigma_1189* with full density NEOs and main belt, with varying levels of random noise.

| Noise Level | $1\times$ | $2\times$ | $5\times$ |
|--|-----------|-----------|-----------|
| Synthetic detections ($\times 10^6$) | 14.1 | 14.1 | 14.1 |
| False detections ($\times 10^6$) | 14.7 | 29.4 | 73.7 |
| Det. ratio (Real/False) | 0.96 | 0.48 | 0.19 |
| Total tracklets ($\times 10^6$) | 8.1 | 11.2 | 28.2 |
| Tracklet Ratio (Real/False) | 2.1 | 1.0 | 0.25 |
| Tracklet CPU (hrs, w/8 cores) | 4.3 | 5.2 | 12.1 |

5. SUMMARY

We have described the motivation and approach for our study to quantify and validate LSST’s NEO search performance. Our key study results will be

- Quantification of the rate of false detections that causes MOPS to falter in linking real objects and compare this with the false detection rate that can be reasonably anticipated, based on estimates from the study collaborators.
- Quantification of LSST’s NEO search and discovery performance, both with the evolving baseline cadence and modest adjustments to that baseline, as well as with hypothetical NEO-optimized search cadences.
- Based on the foregoing results, provide an overall assessment of the likely performance of LSST in terms of NEO search and discovery.

ACKNOWLEDGMENTS

We are grateful for the cooperation of the LSST Project through our consultations with Željko Ivezić, Lynne Jones, and Mario Jurić of the Univ. of Washington. And we thank George Helou and Frank Masci of Caltech’s Infrared Processing and Analysis Center for fruitful discussions and collaboration. This work was conducted at the Jet Propul-

sion Laboratory, California Institute of Technology under a contract with the National Aeronautics and Space Administration.

REFERENCES

- [1] Ivezić, Ž., et al., 2014, “LSST: from Science Drivers to Reference Design and Anticipated Data Products,” <http://arxiv.org/abs/0805.2366>
- [2] Denneau, L., et al., 2013. Publications of the Astronomical Society of the Pacific, 125, 357–395.
- [3] Delgado, F., Saha, A., Chandrasekharan, S., Cook, K., Petry, C., Ridgway, S. 2014. Society of Photo-Optical Instrumentation Engineers (SPIE) Conference Series 9150, 915015.
- [4] Bottke, W. F. et al., 2000. Science 288, 2190–2194.
- [5] Gray, T., et al., 2011. Publications of the Astronomical Society of the Pacific, 123, 423–447.
- [6] Granvik, M., et al., 2013. AAS/Division for Planetary Sciences Meeting Abstracts, 45, #106.02
- [7] Kaiser, N. 2004: The likelihood of point sources in pixelated images. Pan- STARRS internal document PSDC-200-010-00 available upon request.

BIOGRAPHY



Steve Chesley received his B.S. and M.S. degrees in Aerospace Engineering from Texas A&M University in 1986 and 1993, and his Ph.D. in Aerospace Engineering from the University of Texas at Austin in 1998. He is currently a Senior Research Scientist in the Solar System Dynamics Group at NASA’s Jet Propulsion Laboratory, where he led the development of Sentry, JPL’s automated asteroid impact monitoring system. His long-term research focus is on impact hazard assessment and precision orbit determination and ephemeris prediction for small solar system bodies.



Peter Vereš received his M.S. degree in Physics and Astronomy in 2006 and Ph.D. degree in Astronomy and Astrophysics in 2010 from the Comenius University in Bratislava, Slovakia. From 2011 to 2014 he worked as a Pan-STARRS1 MOPS Postdoctoral Fellow at University of Hawaii. He currently works as a Caltech Postdoctoral Scholar at NASA’s Jet Propulsion Laboratory.

His research activities include NEO survey simulations and search performance, data mining for precovery and follow-up of NEO observations, and physical properties of asteroid populations derived from big data and surveys.